The International Journal of Advanced Manufacturing Technology (2018) 97:1–11
https://doi.org/10.1007/s00170-018-1803-6

ORIGINAL ARTICLE

Optimum curved die profile for tube drawing process with fixed conical plug

Nima Dabiri Farahani[1] · Ali Parvizi[1] · Ali Barooni[1] · Sina Anvari Naeini[1]

Received: 22 September 2017 / Accepted: 13 February 2018 / Published online: 26 March 2018

Abstract

Wide applications of tube drawing process with using a fixed conical plug in manufacturing of thin-walled tubes have convinced the researchers to investigate and optimize this process in the past years. Current study deals with presenting an optimum curved die profile utilized in tube drawing process with fixed conical plug. Minimizing the required tensile stress in the process as well as reducing the stress which is applied to the die and plug has been considered as objectives of this study. Considering work-hardening behavior of material, the drawing stress of the process is analyzed based on incremental slab method theory. In addition to, plain strain condition is applied through the thin-walled tube. Furthermore, the obtained optimum die profile has also been simulated using ANSYS Workbench 18.0 and the results were compared with those of analytical method. It is found that the die profile could be determined based on the mechanical properties of the workpiece, reduction of cross section area, plug angle, and coefficients of friction. Results demonstrate that by applying an optimum die profile, the required tension stress in tube drawing process could considerably be reduced comparing to the same process with conical die profile.

Keywords Tube drawing · Curved die profile · Slab method · Optimization · FEM

Nomenclatures

h	Wall thickness of the tube (m)
h_1, h_n	Initial and final wall thicknesses of the tube, respectively (m)
h_i	Wall thickness of the tube at entry of section i (m)
k	Shear yield stress of tube Material (Pa)
m	Work-hardening component of tube material
n	Number of sections
r	Reduction in area (%)
A_1, A_n	Initial and final areas of the tube (m^2)
D_{I1}, D_{In}	Initial and final inner diameters of the tube, respectively (m)
D	Equivalent inner diameter of the tube (m)
K	Strength coefficient of tube material (Pa)
L	Contact length between tool and work metal (m)
P_1, P_2	Pressure in the die and plug, respectively (Pa)
P	Equivalent pressure of the die and plug (Pa)
S	Yield stress of tube material under plane strain condition (Pa)
Y	Uniaxial yield stress of tube material (Pa)
α	Semi-cone angle (Rad)
α_i	Semi-cone angle of section i (Rad)
β	Semi-cone angle of the inner plug (Rad)
Δ	Deformation zone geometry parameter
$\overline{\varepsilon}$	von-Mises equivalent strain
$\overline{\varepsilon}_i$	von-Mises equivalent strain of section i
ε_i	Strain in z direction of section i
ε_{ti}	Total strain in z direction of section i
μ_1, μ_2	Friction coefficients between tube-die and tube-inner plug, respectively
σ	Axial stress in z direction (Pa)
σ_i	Axial stress in z direction at the entry of section i (Pa)
σ_1, σ_n	Axial stresses in z direction at the entry and exit of die, respectively (Pa)
φ	Redundancy factor

✉ Ali Parvizi
aliparvizi@ut.ac.ir

[1] School of Mechanical Engineering, College of Engineering, University of Tehran, Tehran, Iran

1 Introduction

Drawing is a process in which the area of a wire or tube is reduced as it passes throw a series of dies. Tube drawing is one of the metal-forming processes that is widely used in manufacturing seamless pipes. Tube drawing with fixed mandrel, floating mandrel, moving mandrel, and without mandrel are four basic procedures for cold tube drawing. Mandrels and plugs play a key role in maintaining the constant inner diameter and preventing wrinkles during the drawing process. During the drawing process, tube diameter decreases until desired value is achieved. For greater amounts of reduction in diameter, the process would be carried out in several passes with annealing during each pass [1].

Analyzing of a drawing process is carried out based on several methods such as Slab Method (SM), Upper Bound Method (UBM), Finite Element Method (FEM), and finally through experimental investigation. Since slab method is straightforward to be implemented in the mechanical processes, this method along with numerical methods has been widely used in analytical researches. Forging, rolling, drawing, and extrusion are the processes which mainly investigated using slab method. Investigation of ring-rolling process was carried out by Parvizi et al. [2]. They considered non-uniformity of normal and shear stresses through the vertical sides of slabs. In addition, analytical solution for three-dimensional asymmetrical wire-rolling process was presented by Parvizi et al. [3]. They calculated pressure, force, and torque in the process.

Sandwich-rolling process was studied by Wang et al. [4]. The phenomenon of considering two different thicknesses of outer layers was investigated using slab method. Results were compared with experimental data of other authors. Rolling of unbounded clad sheet was investigated by Afrouz and Parvizi [5]. They considered constant shear friction model and non-uniformity of shear stresses as well as uniformity of normal stresses in each slab. Parvizi and Afrouz [6] also developed a new solution for analysis of asymmetrical clad sheet bounded before rolling process.

Afrasiab [7] presented an approach to improve die design in the radial forging process of tube without a mandrel. Based on FEM and a novel slab analysis, he presented a curved die profile in order to optimize the process efficiency and overcome the process difficulties. Investigation of forging three-layer clad sheet was carried out by Pavizi et al. [8]. Considering the effect of shear forces, they evaluated the pressure and force during the process. In addition, they performed a finite element simulation as well as experimental study to verify the process.

Reviewing the literature of drawing process, Swiatkowski et al. [9] studied the tube drawing process with movable mandrel. Palegnat et al. [10] investigated cold drawing of thin-walled tubes by means of experiment and finite element analyses. Rubio et al. [11, 12] studied the drawing process with fixed conical plug using energetic analysis, slab method, and finite element method. They discussed the effects of changing die and plug angle based on results from slab method. Orhan [13] investigated the effect of the semi die and plug angle on cold tube drawing with fixed plug utilizing FEM simulation. He determined the optimum die angle to form AISI 1010 material for the tube.

Considering optimization of the process parameters, optimization of the die profile in hot extrusion process was carried out by Wifi et al. [14] which led to determination of a second-order polynomial curve for the die profile. In the same line, Noorani-Azad et al. [15] made an experimental and numerical studies of optimum die profile in cold forward rod extrusion of aluminum. Taking an industrial point of view in to account, Lee et al. [16] studied the die shape design in drawing process using finite element analysis as well as the flexible polyhedron search method. Having modeled the die by Bezier curve, they carried out an experimental study using the optimized tool. Using design of experiment, an optimal design of process parameters considering rectangular parts was carried out by Salehi et al. [17]. Making use of both arc and Bezier curves, the optimization of die design in single pass steel tube drawing with large strain deformation was investigated by Sheu et al. [18]. Design of experiment method and cost were respectively considered as methodology and objective function in aforementioned study.

While all previous contributions are experimental, this paper aims to analytically optimize die profile by means of slab method utilized in thin-walled tube drawing process ($h_i \ll D$) with fixed conical plug. Taking the work hardening of the work material into account, minimizing the necessary drawing stress of the process is chosen as the objective function. Moreover, Coulomb friction model [19] is assumed at both interfaces of tube-plug and tube-die, while constant and different coefficients are applied to further investigate the parameters. Finally, finite element analysis is also implemented in order to compare the analytical and numerical results. The optimum die profile would lead to lower cost and time efficient optimization of the process. The present close form approach can be utilized as an efficient tool in the related industries in order to lower the tension stress in tube drawing process.

2 The incremental slab analysis for curved die profiles

An analytical solution is developed to determine the optimum curved die profile in thin-walled tube drawing process. As shown in Fig. 1, the deformation zone between inlet and exit of the curved die is divided into n sections. The die profile however possesses $n-1$ slabs which they are analyzed similarly as a small conical die with semi-cone angle of α.

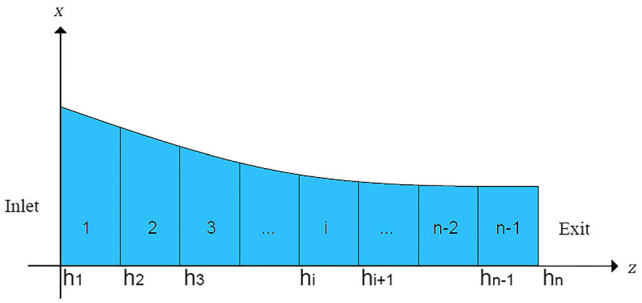

Fig. 1 Divisions of the optional die profile

Geometrical parameters of die, plug, and tube are illustrated in Fig. 2. During the process, geometry of the conical inner plug will not be changed. Considering the tube shape, it is evident that the inner diameter of the tube is assumed to be almost constant, while there will be considerable change in the wall thickness of the tube. Therefore, as presented by Rubio [12], the behavior of the thin-walled tube in drawing process could be described as a plane strain condition. This assumption causes the metal to be flowed in a direction parallel to x-z plane during the process.

2.1 Governing equations

Reduction in area of the tube is defined as follows:

$$r = \frac{A_1 - A_n}{A_1} \tag{1}$$

In the most of the industrial processes, the change in the inner diameter of the tube is negligible and it could be taken as a constant. Also, wall thickness of the tube is too small compared to the inner diameter, i.e.:

$$h_i \ll D_{I1} \approx D_{In} \approx D \tag{2}$$

Consequently, Eq. (1) can be simplified as the following for the thin-walled tube drawing process [12]:

$$r = 1 - \frac{h_n}{h_1} \tag{3}$$

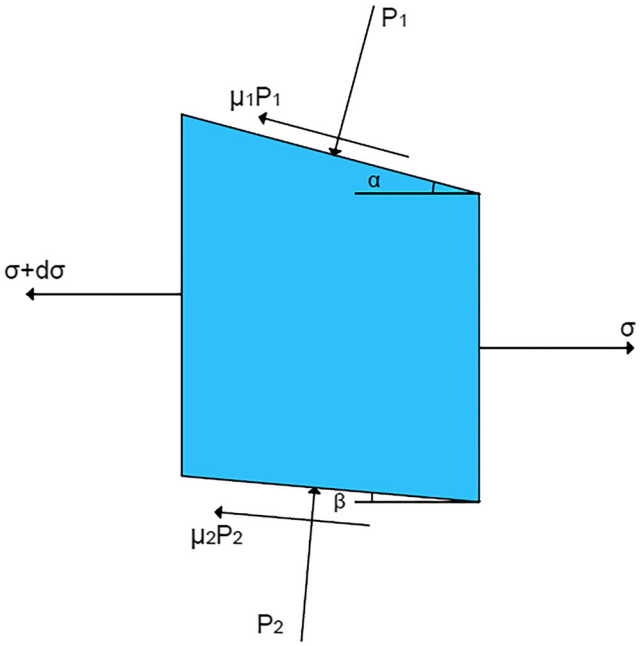

Fig. 3 stress distribution in an arbitrary element of section i

Figure 3 illustrates the stress distribution in arbitrary element of section i. Equilibrium equation in z direction in each element of optional curved profile is obtained as follows:

$$\begin{aligned} &\sigma h - (\sigma + d\sigma)(h + dh) - P_1 tg(\alpha) dz \\ &\quad + P_2 tg(\beta) dz - P_1 \mu_1 dz - P_2 \mu_2 dz \\ &\quad = 0 \end{aligned} \tag{4}$$

From the geometry, the following relation can be obtained:

$$dh = (tg(\alpha) - tg(\beta)) dz \tag{5}$$

Moreover, equilibrium equation in x direction would yield as the following:

$$P_2 = P_1 \frac{1 - \mu_1 tg(\alpha)}{1 + \mu_2 tg(\beta)} \tag{6}$$

Figure 4 depicts the inverse relationship between die and plug pressures for different values of α, β, $\mu 1$, and $\mu 2$. As it

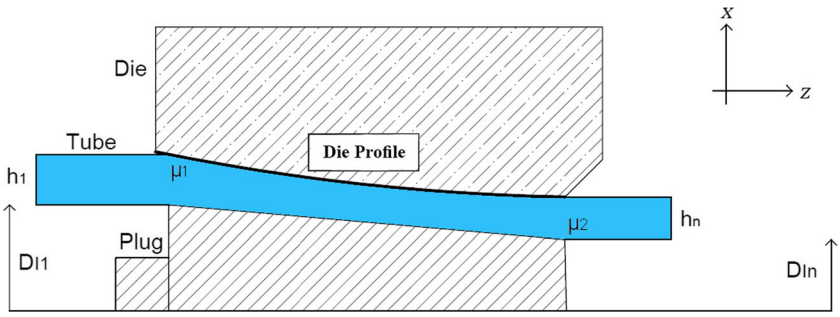

Fig. 2 Geometrical parameters of die, tube, and plug

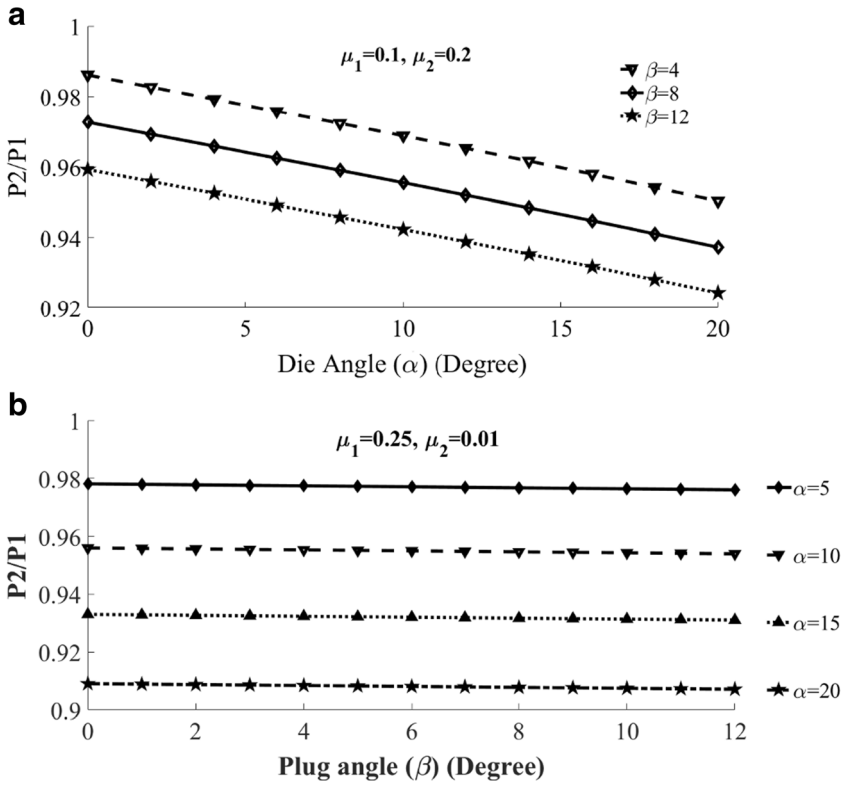

Fig. 4 Ratio P_2/P_1 for different **a** die **b** plug angles

can be seen, variation in plug and die angles do not have considerable effect on the pressure ratio. Hence, plug and die pressures are assumed to be equivalent in this paper. The same assumption was taken into account for the other values of friction coefficient [12]. Therefore:

$$P_2 = P_1 = P \tag{7}$$

Considering equilibrium in x direction as well as neglecting the shear stresses, it is possible to write:

$$\sigma_1 = \sigma \quad , \sigma_2 = -P \tag{8}$$

in which σ_1 and σ_2 are the principle stresses in the z and x directions, respectively. In case of work-hardening condition, von-Mises yield criteria would be written as [19]:

$$\sigma + P = K\overline{\varepsilon}^{\,m} \tag{9}$$

where $\overline{\varepsilon}$ is an equivalent strain.

Substituting Eqs. (5), (7), and (9) into Eq. (4), governing differential equation for stress in each element with work-hardening effect is obtained as:

$$\frac{d\sigma}{B^*\sigma - K\overline{\varepsilon}^{\,m}\left(1+B^*\right)} = \frac{dh}{h} \tag{10}$$

where:

$$B^* = \frac{\mu_1 + \mu_2}{tg(\alpha) - tg(\beta)} \tag{11}$$

Therefore, the governing equation of stress and the corresponding value of B^* for the section i of the die summarized as follows:

$$\frac{d\sigma}{B_i^*\sigma - K\overline{\varepsilon_i}^{\,m}\left(1+B_i^*\right)} = \frac{dh}{h} \tag{12}$$

$$B_i^* = \frac{\mu_1 + \mu_2}{tg(\alpha_i) - tg(\beta)} \tag{13}$$

According to Fig. 1, thicknesses of the wall at the beginning and exit of section i are defined as h_i and h_{i+1}, respectively. The values of i also change from 1 to $n-1$. According to Eq. (3), strain at each section could be determined by:

$$\varepsilon_i = \ln\frac{h_{i+1}}{h_i} \tag{14}$$

where, thicknesses of each section could also be calculated using the following relations:

$$\begin{aligned} h_i &= h_1 + \frac{h_n - h_1}{n-1}(i-1) \\ h_{i+1} &= h_1 + \frac{h_n - h_1}{n-1}(i) \end{aligned} \tag{15}$$

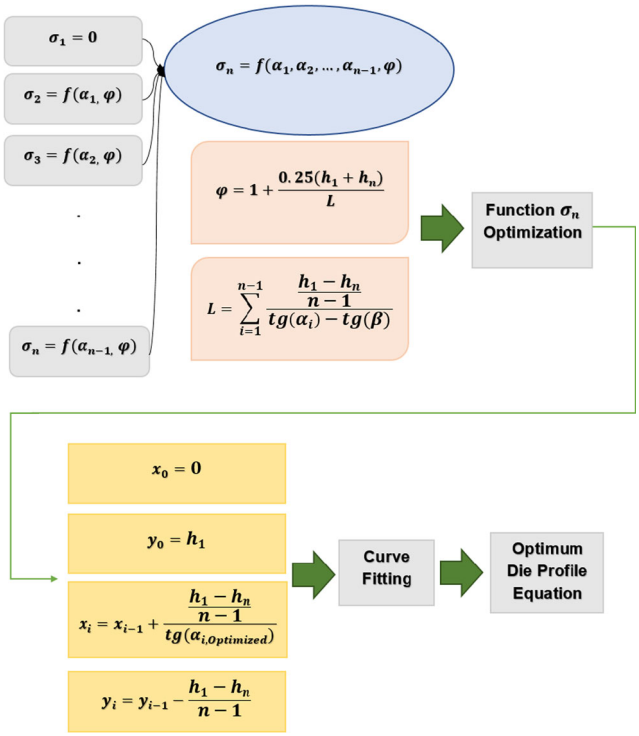

Fig. 5 Flow chart of the procedure to determine optimum die profile

Therefore, Eq. (14) could be rewritten as:

$$\varepsilon_i = \ln \frac{h_1 + \frac{h_n - h_1}{n-1}(i)}{h_1 + \frac{h_n - h_1}{n-1}(i-1)} \tag{16}$$

Moreover, considering the Eq. (3) and Eq. (16), results can be written as follows:

$$\varepsilon_i = \ln \frac{(n-1) - r(i)}{(n-1) - r(i-1)} \tag{17}$$

As it can be seen in Eq. (17), strain in each section is independent of the thickness values at the inlet and exit of the section and it is only a function of reduction in area. Total strain can also be determined as follows [19]:

$$\varepsilon_{ti} = \varphi \varepsilon_i \tag{18}$$

Where φ is a redundancy factor that is calculated for plane strain drawing based on the following Eq. (19):

$$\varphi = 1 + 0.25\Delta \tag{19}$$

Furthermore, the deformation zone geometry parameter, Δ, is defined as:

$$\Delta = \frac{h}{L} \tag{20}$$

where L is the contact length between tool and work metal in the die and h is the mean thickness of tube which is obtained by:

$$h = \frac{2h_n + 2h_1}{2} = h_n + h_1 \tag{21}$$

In order to obtain the equivalent von-Mises strain in section i, the history of the strain from the die inlet to the section exit should be considered. Hence, considering the plane strain behavior of the material, $\overline{\varepsilon}_i$ is:

$$\overline{\varepsilon}_i = \frac{2}{\sqrt{3}} \ln \frac{h_1}{h_{i+1}} \tag{22}$$

Using Eqs. (3) and (15), the following relation is obtained:

$$\overline{\varepsilon}_i = \frac{2}{\sqrt{3}} \ln \frac{(n-1)}{(n-1) - r(i)} \tag{23}$$

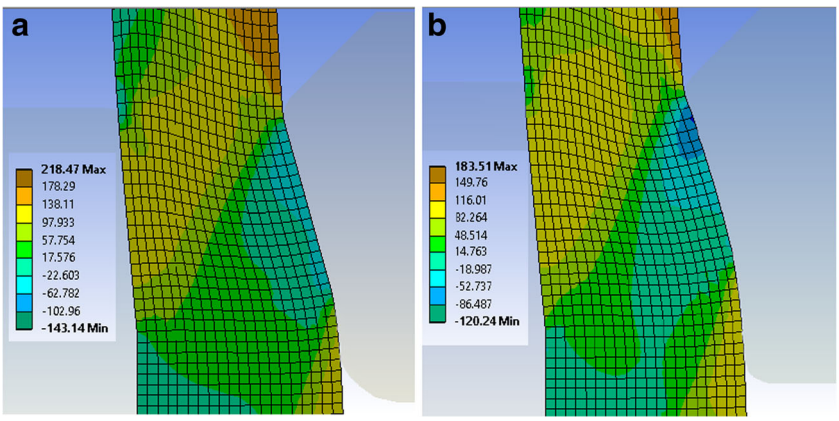

Fig. 6 Deformed mesh in case of **a** conical die **b** optimum curved die

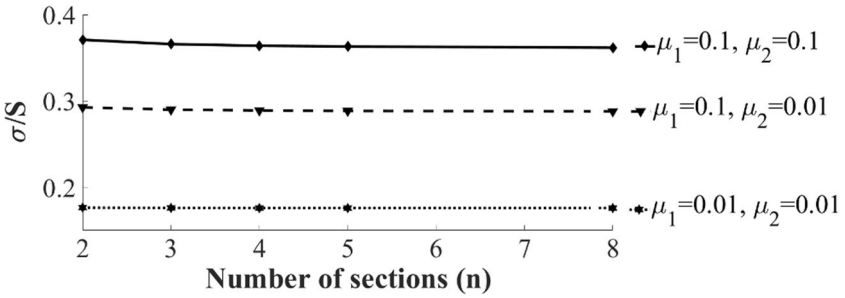

Fig. 7 Effects of coefficients of friction on dimensionless drawing stress (perfectly plastic behavior, i.e., $m = 0$) for $r = 0.1$

With fully determined process parameters, the boundary conditions for Eq. (12) are summarized as:

$$\begin{aligned} h = h_1 &\rightarrow \sigma = \sigma_i \\ h = h_{i+1} &\rightarrow \sigma = \sigma_{i+1} \end{aligned} \tag{24}$$

Considering the given boundary conditions, direct integration of Eq. (12) is given as follows:

$$\sigma_{i+1} = K\overline{\varepsilon_i}^{m}\left(\frac{1+B_i^*}{B_i^*}\right) + \left(\sigma_i - K\overline{\varepsilon_i}^{m}\left(\frac{1+B_i^*}{B_i^*}\right)\right) exp\left(B_i^* ln\frac{h_{i+1}}{h_i}\right) \tag{25}$$

The expression is valid for any μ and K values. However, the simplest solution is obtained when these parameters are remained constant during the process.

Substituting $\varphi\varepsilon_i$ into Eq. (25) will result into:

$$\frac{\sigma_{i+1}}{K} = \overline{\varepsilon_i}^{m} B_i + \left(\frac{\sigma_i}{K} - \overline{\varepsilon_i}^{m} B_i\right)\exp\left(B_i^*\varphi\varepsilon_i\right) \tag{26}$$

where:

$$B_i = \frac{1+B_i^*}{B_i^*} \tag{27}$$

In case of elastic perfectly plastic behavior of the material, i.e., $m = 0$, strength coefficient K in Eq. (26) can be replaced with yield stress under plane strain condition which is defined as follows [19]:

$$K = S = 2k = \frac{2}{\sqrt{3}}Y \tag{28}$$

3 Determination of optimum die profile

In tube drawing process, stress at the inlet of the die is assumed to be zero, i.e., $\sigma_1 = 0$. Considering constant coefficients of friction, μ_1 and μ_2, strength coefficient K, work-hardening component m, reduction in area r, and the number of sections n, as the input parameters, stress in section 2, σ_2, can be defined by semi-cone angle of this section α_1 and redundancy factor φ. Substituting σ_2 in Eq. (26), stress in section 3, σ_3, would be defined using values of α_1, α_2, and φ. The procedure is repeated for other sections until $i = n - 1$. In this case, the drawing stress σ_n, as the objective function, is defined by parameters α_1, α_2, ..., α_{n-1}, and φ. At first, the redundancy factor φ, is unknown, since the deformation zone geometry parameter Δ, would be determined from the die profile, which is the aim of the design. To solve this issue, the contact length L, between work metal and die, is taken the sum of contact lengths in each section. So, this parameter can be calculated from the geometry of the problem, i.e., $L = \sum_{i=1}^{n-1}$

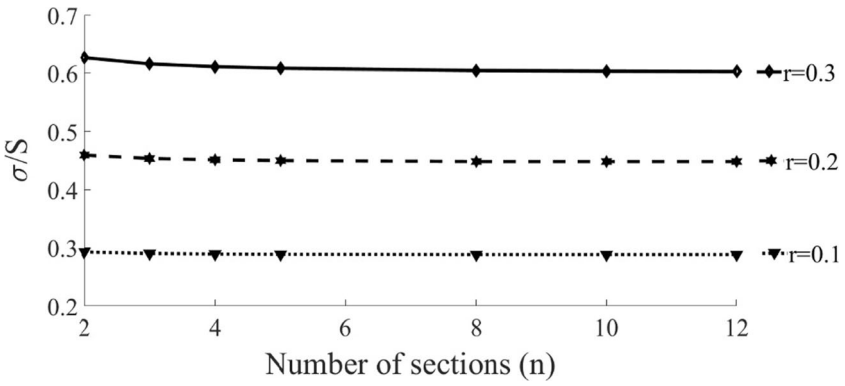

Fig. 8 Effects of reduction in area on dimensionless drawing stress (perfectly plastic behavior, i.e., $m = 0$) for $\mu_1 = 0.1$, $\mu_2 = 0.01$

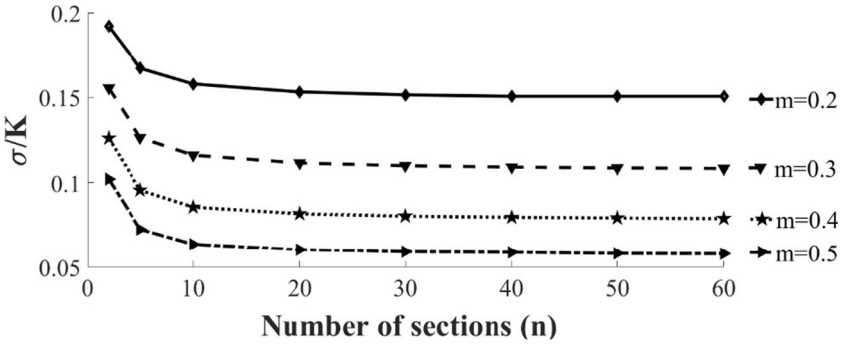

Fig. 9 Effects of work-hardening component on dimensionless drawing stress (work-hardening behavior) for $r = 0.1$, $\mu_1 = 0.1$, $\mu_2 = 0.01$

$\frac{\frac{h_1-h_n}{n-1}}{tg(\alpha_i)-tg(\beta)}$ and the drawing stress would be a function of semi-cone angles of each section. Optimum value of drawing stress and semi-cone angles of each section, which is considered in the range of 1 to 89 degrees, can be calculated using a developed computer program. Since the die profile obtained by the defined algorithm is not linear, the result was curve fitted using a second-order polynomial method. This procedure is also represented in Fig. 5.

4 Finite element simulation

In order to evaluate results obtained from the slab method, thin-walled tube drawing process is entirely simulated using finite element software ANSYS Workbench 18.0 [20], as it is illuminated in Fig. 6. Considering simple geometry of the process, a 2D axisymmetric model is used to simulate the process in order to minimize the required time. Moreover, considering the nonlinear behavior of the process, an explicit dynamic FE analysis was performed. Plug and die are modeled as rigid in this simulation. Low-carbon steel with a yield strength of 245 MPa at room temperature is considered as simulation material. To investigate the condition, both work hardening and perfectly plastic material behaviors are considered in the simulation. In case of work hardening, the behavior of the material is modeled by $\sigma = 550\varepsilon^{0.22}$, while the yield stress is considered to be 245 *MPa* for the perfectly plastic case.

Eight-node quadrilateral element is used for meshing the simulated work metal and four-node rigid elements are used for the die and plug. The approximate size of seeds in the deformation zone was 0.1 mm, while the worst quantity of the aspect ratio was 1.25 at this zone. Also, Coulomb friction model is considered in the simulation. Furthermore, short-length parts were added to the plug and die so as to guide the material throw the die. These parts are neglected in the slab method analysis. For boundary conditions, the plug and die were kept fixed and the tube is passed through the die with a constant velocity of 30 mm/s. Finally, the drawing stress was obtained as the objective function using normal stress values in z direction. The convergence rate for the calculation was acceptable, and the duration of each numerical analysis was about 2 h. Higher process velocities could decline the duration of the analysis while almost the same results are obtained at the steady-state condition.

5 Results and discussion

5.1 Results of slab method analysis

Results obtained from slab method analysis, i.e., Eq. 26, are presented and investigated in this section. Effects of changing

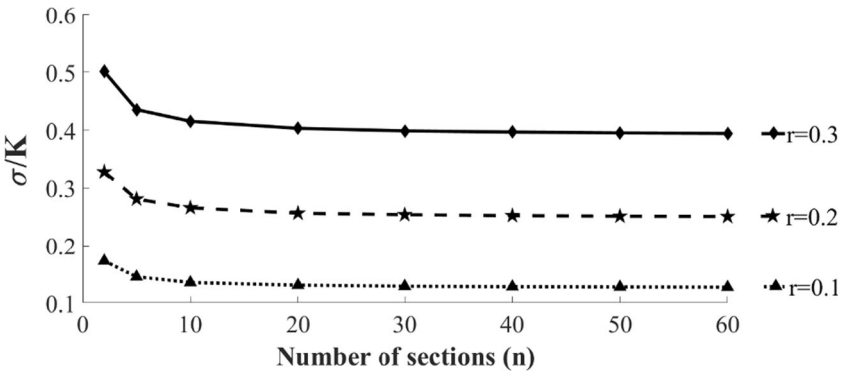

Fig. 10 Effects of reduction in area on dimensionless drawing stress (work-hardening behavior) for $m = 0.25$, $\mu_1 = 0.1$, $\mu_2 = 0.01$

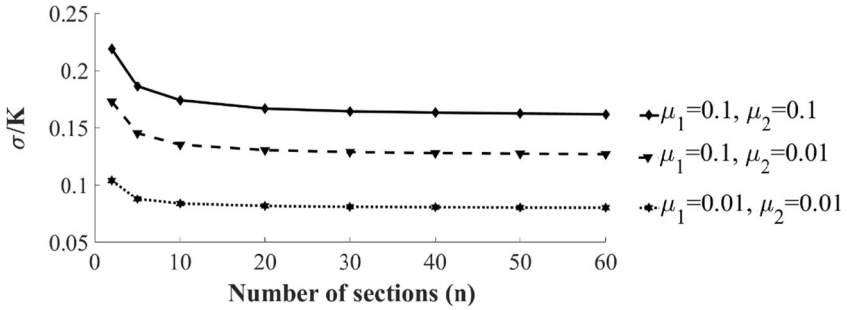

Fig. 11 Effects of coefficients of friction on dimensionless drawing stress (work-hardening behavior) for $m = 0.25$, $r = 0.1$

reduction in area, hardening component, and plug angle as well as coefficients of friction between tube-die and tube-plug are discussed in this section. This set of parameters is chosen according to handbook of metal forming [19] as the most effective parameters in the drawing process. Then, to compare the results of drawing process with those of extrusion process [14, 15], the effect of these parameters is fully studied.

Taking plane strain yield stress S into account, the dimensionless drawing stress of the process versus number of sections are illustrated in Fig. 7. In this figure, material is considered to have an elastic perfectly plastic behavior. Moreover, different coefficients of friction between plug-tube and die-tube are considered to investigate the consequences. According to the figure, dimensionless drawing stress converges to its optimum value as the number of sections increases. In case of constant yield stress, the optimum drawing stress value is close to that one while the die profile is conical with optimum semi-cone angle. However, by applying more sections, the more accurate curve can be fitted. Actually, conical die shape could be obtained by considering two sections (one slab) for division. In addition, the drawing stress also increases when the friction increases at interfaces of both die and plug. In this case, the work stablished by friction is risen. It should be noted that based on Eq. (13), the effects of increasing each coefficient of friction are compliant with those demonstrated in the figure.

Figure 8 demonstrates the effects of reduction in area on the drawing stress in different number of sections. It is apparent that by utilizing 10 to 12 sections, the value of dimensionless drawing stress slightly converges to its optimum value. It is clear that the drawing stress increases for higher amount of reduction in area. This phenomenon also leads to longer contact length between work metal and die. According to the figure, it is obvious that for every 0.1 increase in reduction in area, there is an approximately 0.2 growth in value of dimensionless drawing stress. Since the optimization is carried out based on minimizing the drawing stress with respect to a specific amount of reduction in area, this value remains the same with die profile optimization. Also, the maximum reduction in area is limited to approximately 0.4 while the more amounts of reduction hinder the tube movement and consequently, lead to failure of the tube since dimensionless drawing stress tends to be 0.866 [12, 19].

Considering Fig. 9, dimensionless drawing stress is plotted for different number of sections while work hardening is considered in the work metal. In this case, the drawing stress significantly decreases while the number of sections increases. Thus, it is suggested to use dies with optimum curved profile in the primary passes of the tube drawing process, in which the effect of work hardening is more noticeable. Moreover, the drawing stress decreases as the work-hardening component increases. In other words, increasing work-hardening component causes the softening of the material, and therefore, less load is required for the process to be carried out. Also, the change in the value of the optimum drawing stress decreases as a consequence of the increase in the hardening component. Actually, this plot is drawn for 50 sections of the die, while the change in the stress value is negligible after specific number of

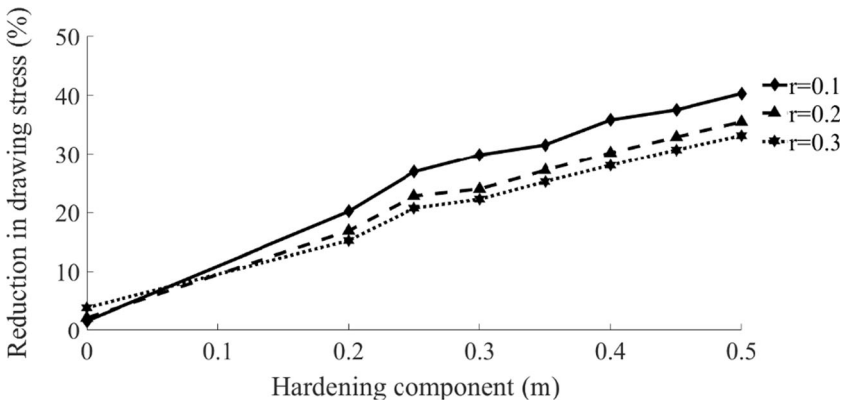

Fig. 12 Effects of hardening component on reduction in drawing stress with respect to different amounts of reduction in area for $\mu_1 = 0.1$, $\mu_2 = 0.01$

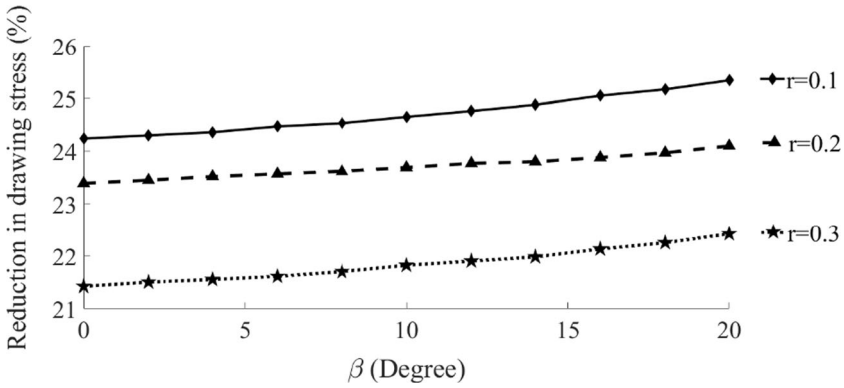

Fig. 13 Effects of semi-cone angle of the inner plug β on drawing stress reduction percentage with respect to different amounts of reduction in area for $m = 0.25$, $\mu_1 = 0.1$, $\mu_2 = 0.01$

sections. In this condition, all the stress values are about 99% of their optimum values that demonstrate the accuracy of the procedure. Increasing the number of sections makes the process similar to a multi-pass cold drawing process, in which lower amounts of overall von-Mises stress and drawing load were reported for different materials as well as different final shapes [21, 22].

Considering work-hardening behavior, dimensionless drawing stress is plotted for different number of sections with three different amounts of reductions in Fig. 10. Based on this figure, the drawing stress increases for higher quantities of reductions in area. The trend is the same for both perfectly plastic and work-hardening materials. Here, in order to avoid large plastic deformations, the angle of each section is limited to 15°. As shown in the figure, the convergence to the optimum value of drawing stress is achieved after 10 to 20 die sections for all three cases. As it can be seen, 0.1 increase in reduction in area approximately increases 0.15 value of dimensionless drawing stress which in turn would lead to more amount of reduction, i.e., approximately 0.6 in area in comparison with the conical plugs. In this case, the limiting value of the stress is fully depended on the strength ratio of the material.

Figure 11 shows the effects of friction coefficient on dimensionless drawing stress with respect to number of sections. It is shown that increasing the friction causes higher optimum drawing stress as a result of more work required to overcome friction. The trend is the same for both coefficients of friction at the interfaces of tube-die and tube-plug. Furthermore, it can be described that about 12% drop in drawing stress value is achieved by decreasing the summation of friction coefficient value to 0.2. The lower value shows the smoother die profile after the optimization process. As a consequence, the tool life will increase since the tool will experience less wear during the process. Moreover, the die profile, along with reduction of area, friction coefficients, and plug shape, have the main effect on residual stresses in cold drawing process [23, 24]. The desired values of coefficients of friction can be achieved using appropriate lubrication and smooth plug.

Figure 12 illustrates the effects of hardening component on drawing stress reduction for different amounts of reduction in area. As it can be seen, the maximum amount of 45% reduction in drawing stress can be achieved by die profile optimization. This value is 10 to 25% for the most of the work metals utilized in the process. In all cases, drawing stress reduction is calculated with respect to the equivalent optimum conical die profile. It is shown that higher percentage of reduction in drawing is obtained in case of bigger amount of work-hardening component. This would be a consequence of work metal softening as the hardening component increases. However, this value decreases while the reduction in area increases. Similarly, in case of perfectly plastic condition, this value increases with almost the same trend.

Effects of semi-cone angle of the inner plug β on drawing stress reduction percentage with respect to different amounts

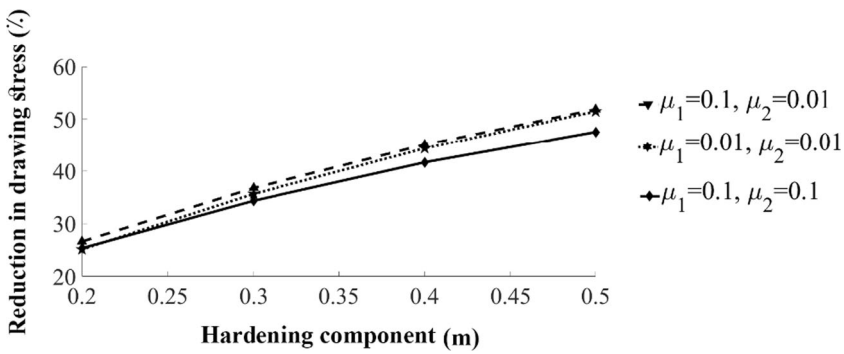

Fig. 14 Effects of hardening component on drawing stress percentage with respect to different friction coefficients for $r = 0.1$

Table 1 Parameters of the FEM simulation

Trial no.	μ_1	μ_2	β (*deg.*)	r (%)	σ (*MPa*)
1	0.1	0.01	5	20	$550\bar{\varepsilon}^{0.22}$
2	0.1	0. 1	5	10	$550\bar{\varepsilon}^{0.22}$
3	0.1	0.01	8	20	245

of reduction in area are demonstrated in Fig. 13. As shown, maximum amount of 25% reduction in drawing stress can be achieved while using conventional plug angles. It is shown that when the plug angle increases, the drawing stress reduction percentage increases slowly. In fact, the optimization causes to have approximately a constant value of drawing stress reduction percentage for each quantity of reduction in area. However, the optimum die profile is different for different plug angles. The value of the reduction in drawing stress also decreases while the reduction in area increases. Nevertheless, for a specific amount of reduction in area, the approximate value of 1% difference in the reduction in drawing stress can be achieved by changing inner plug semi-cone angle from 0 to 20°. However, the plug semi-cone angle as well as die profile is a crucial parameter in outer diameter (OD) dimension tolerances especially in drawing process of high-pressure tubes [25]. They should be applied considering tolerance and damage criteria.

Figure 14 shows the effects of hardening component on drawing stress reduction percentage with respect to different friction coefficients at the interfaces of tube-die and tube-plug. It is shown that the value of the reduction in drawing stress is almost the same for different coefficients of friction after optimization process. In this case, the effect of friction coefficient on drawing stress decreases. It is obvious that the effect of changing both coefficients of friction is the same in this case. Also, approximately 5 to 10% difference in reduction in drawing stress for higher values of friction can be implied from the figure. This reduction in drawing stress causes the optimization to be more suitable in cases which sufficient lubrication is not possible. Finally, it can also reduce the drawing stress up to 50%.

5.2 Results for finite element analysis

In order to compare the analytical and numerical results, three different cases have been studied by means of finite element simulation. Parameters considered in the simulation are illustrated in Table 1. Comparison between analytical and FEM results is demonstrated in Table 2. $\sigma_{n,\,SM,\,Con.}$ and $\sigma_{n,\,FEM,\,Cur.}$ are drawing stresses for conical and optimum curved die profiles based on the slab method and FEM simulation, respectively. The FEM results are considered to be mean normalized tension stress so as to be compared with those of analytical approach. It should be noted that based on FEM results, the maximum normalized tension stress is greater in value while using optimum curved die profile, which could not be considered in analytical approach. Results from Table 2 show acceptable agreements between analytical and FEM outcomes. The maximum difference between analytical and FEM results for drawing stress percentage reduction is about 6%. Additionally, the obtained stresses from FEM simulation are close to the values calculated by slab method. In this case, the maximum difference between the results is 9%.

6 Conclusions

In this study, the optimum curved die profile for thin-walled tube drawing process with fixed inner plug is presented. The optimization carried out using an incremental slab method and the second-order optimum polynomial die curve was curve-fitted to the analytical results for the first time. Elastic perfectly plastic as well as work-hardening behaviors was considered for material behavior. Moreover, the process is wholly simulated by ANSYS Workbench 18.0 and the results are compared with results of the slab method. Generally, good agreements between the results are achieved. It is concluded that in case of work-hardening behavior of the work metal, optimization would cause significant reduction in drawing stress, i.e., 10 to 25% for most of the work metals utilized in the process. However, in case of elastic perfectly plastic behavior of the metal work, the difference between drawing stresses extracted from conical and optimum curved profile dies is

Table 2 Results of slab method and FEM simulation

Trial no.	$\sigma_{n,\,SM,\,Con.}$ (*MPa*)	$\sigma_{n,\,FEM,\,Con.}$ (*MPa*)	$\sigma_{n,\,SM,\,Con.}$ (*MPa*)	$\sigma_{n,\,FEM,\,Cur.}$ (*MPa*)	$\%Red._{SM}$	$\%Red._{FEM}$
1	187.44	197.14	147.01	161.02	21.56	18.32
2	133.81	128.84	103.98	107.58	22.31	16.51
3	129.4	131.54	128.05	125.76	1.04	4.39

not so considerable. Actually, the maximum amount in this case is 4%. As an industrial point of view, it is suggested to use dies with optimum curved profile in the primary passes of the tube drawing process, in which the effect of work hardening is more noticeable. For the succeeding passes where the work-hardening effect has considerably reduced, the optimum conical profile could also be used. Moreover, more amounts of reduction in area can be used in the process while using optimum drawing stress. Additionally, it could be implied from the obtained plots that the reduction percentage in drawing stress increases while the reduction in area decreases. Moreover, the drawing stress of the process increases with increasing the friction and reduction in area. In addition, although an increase in the plug semi-cone angle value results in higher drawing stress, changing the die profile to optimum curve could be considered as a solution for that. Also, it is concluded that the reduction percentage in drawing stress is approximately independent of coefficients of friction between tube-plug and tube-die in case of using optimum curved die profile.

The drawing stress is a function of material properties, reduction in area, plug angle, and the friction between tube-die and tube-plug in optimum die profile. Along with optimization of die profile, making use of soft materials in the process with higher hardening components would lead to lower amounts of tension stress. Also, reducing the reduction in area and utilizing succeeding passes of the metal drawing as well as lubrication would cause the same advantageous. In addition, smaller plug angles are preferred in the process based on drawing stress reduction results. The optimum curved die profile presented would lead to lower cost and time efficient optimization of the process. The present close form approach can be utilized as an efficient tool in the related industries in order to decrease the tension stress and drawing load in tube drawing process.

Acknowledgements The authors are grateful for the research support of the Iran National Science Foundation (INSF).

References

1. Avitzur B (1968) Metal forming processes and analysis. McGraw-Hill Education, New York
2. Parvizi A, Abrinia K, Salimi M (2011) Slab analysis of ring rolling assuming constant shear friction. J Mater Eng Perform 20:1505–1511
3. Parvizi A, Pasoodeh B, Abrinia K (2015) An analytical approach to asymmetrical wire rolling process with finite element verification. Int J Adv Manuf Technol 85(1–4):381–389
4. Wang HY, Li X, Sun J, Zhang DH (2015) Analysis of sandwich rolling with two different thicknesses outer layers based on slab method. Int J Mech Sci 106:194–208
5. Afrouz F, Parvizi A (2015) An analytical model of asymmetric rolling of unbounded clad sheets with shear effects. J Manuf Process 20:162–171
6. Parvizi A, Afrouz F (2016) Slab analysis of asymmetrical clad sheet bounded before rolling process. Int J Adv Manuf Technol 87:137–150
7. Afrasiab H (2016) Numerical and analytical approaches for improving die design in the radial forging process of tubes without a mandrel. Sci Iran 23(1):167–173
8. Parvizi A, Rezapour O, Safari MA (2016) Theoretical modeling, simulation and experimental studies of al/cu clad sheet forging. Int J Interact Des Manuf 11(3):525–533
9. Swiatkowski K, Hatalak R (2004) Study of the new floating-plug drawing process of thin-walled tubes. J Mater Process Technol 151(1):105–114
10. Palengat M, Changon G, Favier D, Louche H, Linardon C, Plaideau C (2013) Cold drawing of 3161 stainless steel thin-walled tubes: Experiment and finite element analysis. Int J Mech Sci 70:69–78
11. Rubio EM, Gonzalez C, Marcos M, Sebastian MA (2006) Energetic analysis of tube drawing processes with fixed plug by upper bound method. J Mater Process Technol 177(1):175–178
12. Rubio EM (2006) Analytical methods application to the study of tube drawing processes with fixed conical inner plug: Slab and upper bound methods. J Achieve Mater Manuf Eng 14(1–2):119–130
13. Orhan S (2016) Effects of the semi die/plug angles on cold tube drawing with a fixed plug by FEM for AISI 1010 steel tube. 2015 4th Int Symp on Inno Technol in Eng and Sci, pp. 1065–1074
14. Wifi AS, Shalta MN, Abdel-Hamid A (1998) An optimum curved die profile for the hot forward rod extrusion process. J Mater Process Technol 73:97–107
15. Noorani-Azad M, Bakhshi-Jooybari M, Hosseinipour SJ, Gorji A (2005) Experimental and numerical study of optimal die profile in cold forward rod extrusion of aluminum. J Mater Process Technol 164-165:1572–1577
16. Lee SK, Jeong MS, Kim BM, Lee SB (2013) Die shape design of tube drawing process using FE analysis and optimization method. Int J Adv Manuf Technol 66(1–4):381–392
17. Salehi M, Hosseinzadeh M, Elyasi M (2016) A study on optimal Design of Process Parameters in tube drawing process of rectangular parts by combining box–Behnken Design of Experiment, response surface methodology and artificial bee Colony algorithm. Trans Indian Inst Metals 69(6):1223–1235
18. Sheu JJ, Lin SY, Yu CH (2014) Optimum die Design for Single Pass Steel Tube Drawing with large strain deformation. Procedia Eng 81:688–693
19. Hosford WF, Caddell RM (2007) Metal forming: Mechanics and metallurgy. Cambridge University Press, Cambridge
20. Workbench 18.0, ANSYS, Inc., Canonsburg, Pennsylvania
21. Lin Z, Shen B, Sun F, Zhang Z, Guo S (2015) Numerical and experimental investigation of trapezoidal wire cold drawing through a series of shaped dies. Int J Adv Manuf Technol 76:1383–1391
22. Lee IK, Lee SK, Lee CJ, Jeong MS, Lee JW (2016) A new method for predicting drawing load of shape drawing process. Int J Adv Manuf Technol 84:1747–1755
23. Gattmah J, Ozturk F, Orhan S (2017) Experimental and finite element analysis of residual stresses in cold tube drawing process with a fixed mandrel for AISI 1010 steel tube. Int J Adv Manuf Technol 93:1229–1241
24. Foadian F, Carrado A, Pirling T, Palkowski H (2016) Residual stresses evolution in cu tubes, cold drawn with tilted dies - neutron diffraction measurements and finite element simulation. J Mater Des 107:163–170
25. Ahn S, Park J, Won J, Kim H, Kang I, Cho Y, Shin S (2017) An analytical FEM-based study of the drawing process of an ultra-high-pressure common-rail fuel tube. J Mech Sci Technol 31:3389–3396

Publisher's Note